https://doi.org/10.5194/egusphere-2025-1394
Preprint. Discussion started: 9 April 2025

Controls over debris flow initiation in glacio-volcanic environments in the Southern Andes.

Ivo Fustos-Toribio[1], Daniel Basualto[3*], Ardy Gatica[1], Álvaro Bravo-Alarcón[2,1], José-Luis Palma[4], Gabriel Fuentealba[5,2], Sergio A. Sepúlveda[6,7]

[1]Departamento de Ingeniería en Obras Civiles, Facultad de Ingeniería y Ciencias, Universidad de La Frontera. Francisco Salazar #01145, Temuco, Chile.
[2] Programa de Magíster en Ciencias de La Ingeniería, Universidad de La Frontera, Temuco, Chile.
[3]Departamento de Ingeniería Eléctrica, Facultad de Ingeniería y Ciencias, Universidad de La Frontera. Francisco Salazar #01145, Temuco, Chile.
[4]Departamento Ciencias de la Tierra, Facultad de Ciencias Químicas, Universidad de Concepción, Víctor Lamas 1290, Concepción, Chile.
[5]Ministerio del Interior, Temuco, Chile.
[6] Departamento de Geología, Facultad de Ciencias Físicas y Matemáticas, Universidad de Chile, Santiago, Chile
[7] Department of Earth Sciences, Faculty of Science, Simon Fraser University, Burnaby, Canada

Correspondence to: daniel.basualto@ufrontera.cl

Abstract. The southern Andes is an active zone of mass wasting processes. Several conditioning factors could have an impact on the generation of debris-flows, influencing by water storage and slope stability. We assessed the generation of the Ñisoleufu debris-flow, an active area of debris-flow generation, reviewing the interplay between geomorphological, geotechnical and hydrometeorological controls in debris flow dynamics. Our results highlight significant changes in soil moisture content on critical days associated with debris flow events. We revealed that the combination of areas with high water accumulation capacity from local runoff and slopes that capture precipitation effectively were crucial in the generation of debris-flows. Areas with granular volcanic soils acted as storage mediums for water, which, coupled with decreased shear strength, facilitated debris flow initiation. The thin and fine-grained layers of glacial deposits located beneath the volcanic soil, characterized by low hydraulic conductivity, created localized accumulation zones that reinforced the storage capacity of adjacent areas, particularly in pyroclastic volcanic deposits in the release zone. By understanding the combined effects of water accumulation, soil properties, and slope dynamics, this study contributes valuable insights into managing and mitigating debris-flow hazards in vulnerable regions.

1 Introduction

Debris flows have occurred more frequently due to climate change, resulting in an increase in episodes of extreme rainfall (Jakob and Lambert 2009; Lee 2017; Fustos et al., 2017; Dey and Sengupta 2018) and mainly related to fast changes of soil

https://doi.org/10.5194/egusphere-2025-1394
Preprint. Discussion started: 9 April 2025

water content (Fustos et al., 2021). In South America, these common landslide phenomena produce widespread damages, representing a significant threat to human life (Sepúlveda et al., 2006; Sepúlveda and Petley 2015; Vega and Hidalgo 2016; Garcia-Delgado et al. 2022). Consequently, the need to forecast (Fustos et al., 2020a) and mitigate (Fustos et al., 2021b) the effects of these events has become a high priority for governments facing increasing episodes of rainfall-induced landslides (RIL) linked with climate change. An accurate forecast needs precise understanding of the triggering conditions of debris flows. South America has limited knowledge of the conditioning factors and triggering conditions of flows, which reduces the capacity of authorities and stakeholders to propose science-based decisions.

Understanding the impact of debris flows in glacial environments is critical in the Chilean southern Andes, particularly due to the most part of the inhabitants lives there. Changes of precipitation patterns related to climate change, particularly fast and intense rainfall events, could amplify the frequency and magnitude of debris flows (Fustos et al., 2022). An increase of extreme hydrometeorological events affecting slopes in glacial settings is observed, whose mechanical properties and geomorphology have evolved since the Last Glacial Maximum (Fustos-Toribio et al., 2021; Somos-Valenzuela et al., 2020; Ochoa-Cornejo et al. 2025). Despite the significance of these events to the population, considerable uncertainty remains about how the interaction between volcanic-derived soils over glaciar landforms will respond to extreme hydrometeorological events.

The landslide generation from extensional failures to surface deformation stands out, mainly due to gravity and surface erosion in high precipitation environments (Xie et al, 2020; Yi et al, 2021). Over time, these failures expand and deepen, weakening the soil and predisposing it to landslides, especially under water-saturated conditions or heavy rainfall (Fustos et al., 2017; Wang et al., 2024). The capacity to oversee these extensional failures in remote areas close to roads is an open question yet, mainly in South America. Large landslides can, under certain conditions, transform into debris flows when the slid material mixes with water, increasing its fluidity like the Villa Santa Lucia event in the Chilean Patagonia (Somos-Valenzuela et al., 2020). These debris flows are fast and destructive, capable of transporting large amounts of material and causing significant damage to infrastructure and ecosystems, as well as posing a serious hazards to nearby communities (Hirschberg et al., 2021).

The occurrence of debris flows in volcanic environments is a subject of significant scientific interest (Cheung & Giardino, 2023), primarily due to the intricate nature of volcanic soils and their inherent textural variability (Thompson et al., 2023), which directly impacts water content dynamics. In the Southern Andes region, there remains a conspicuous lack of understanding regarding how these textural variations influence the hydraulic response of these soils during extreme hydrometeorological events. Over the past four decades, this area has witnessed substantial volcanic activity (Moreno-Yaeger et al., 2024), resulting in extensive deposition of tephra that has significantly contributed to the heightened occurrence of debris slides and debris flows (Korup et al., 2019). Despite these recurrent occurrences, substantial gaps persist in comprehending the variability of textural and hydraulic properties of volcanic soils under the influence of extreme hydrometeorological events.

Previous studies suggested the need to seek and address the textural and hydraulic properties of volcanic soils, constraining the hydraulical and geomechanical conditions that enable the debris flow generation (Fustos et al., 2021; Kostynick et al., 2022). These constraints become essential to generate accurate planning over the territory, allowing to save lives and develop accurate early warning systems.

https://doi.org/10.5194/egusphere-2025-1394
Preprint. Discussion started: 9 April 2025

Debris flows are influenced by soil hydraulic characteristics and the intensity/duration of rainfall events (Singh and Kumar, 2021), in which rainfall intensities serve as crucial predictors in mountainous regions (Chang et al., 2017; Fustos-Toribio et al., 2022). Moreover, coarse-grained volcanic soils exhibit transient increases in pore pressure during intense rainfall events (Huang et al., 2012). Conversely, fine-grained soils with low infiltration rates do not experience significant changes in the pore pressure, generating failures due to decreased soil shear strength (Dahal et al., 2008; 2011). Hence, understanding soil composition and granulometric features is pivotal in assessing debris flow susceptibility worldwide.

In this paper, we analyse the precursory surface deformation related to tensile cracks leading to the Ñisoleufu debris flow event (May 31st, 2021). We utilised a multi-temporal InSAR approach with Sentinel-1 C-band SAR data, enabling us to create time series plots of deformation before the landslide and compare them with available daily precipitation records from nearby weather stations and satellite measurements. By combining remote sensing data, weather records, and soil laboratory analyses, we aim to provide valuable insights into the factors leading to such events and, consequently, improve hazard assessment and management in zones with soils derived from explosive volcanic events.

2 Study area

Debris flows are the most common manifestation of mass wasting triggered by precipitation in the Southern Andes due to the soil heterogeneity and geological features, providing a unique opportunity to study the relationship between extreme rainfall and debris flows. Recent events become a significant geological hazard, especially in steep zones near alluvial plains where human settlements are often established (Fustos et al., 2017; Fustos-Toribio et al., 2021). On May 31st, 2021, a very fast debris flow was triggered due to extreme rainfall affecting houses and blocking the CH-201 route in the Ñisoleufu zone, southern Chile, generating economic losses in a vulnerable rural area **(**Figure 1**)**. The deposit mainly consisted of rock blocks and trunks covered by a thin layer of debris. Much of the debris flow fell into the adjacent Calafquén lake (Figure 1), causing a small tsunami. The event was extremely rapid, based on the classification proposed by Hungr et al. (2014), with a speed estimated to be over 3 m/s . Stand out that the debris flow experienced reactivation events on June 19, 2023, and again on June 28, 2024. The debris flow was deposited in a flat area of the valley (slopes between 0-20°), flowing into Lake Calafquén. The presence of landslide deposits and old flows in the vicinity of the lake (Figure 1**A**; geologic map [Ha]) suggests that this phenomenon is common in the area.

https://doi.org/10.5194/egusphere-2025-1394
Preprint. Discussion started: 9 April 2025

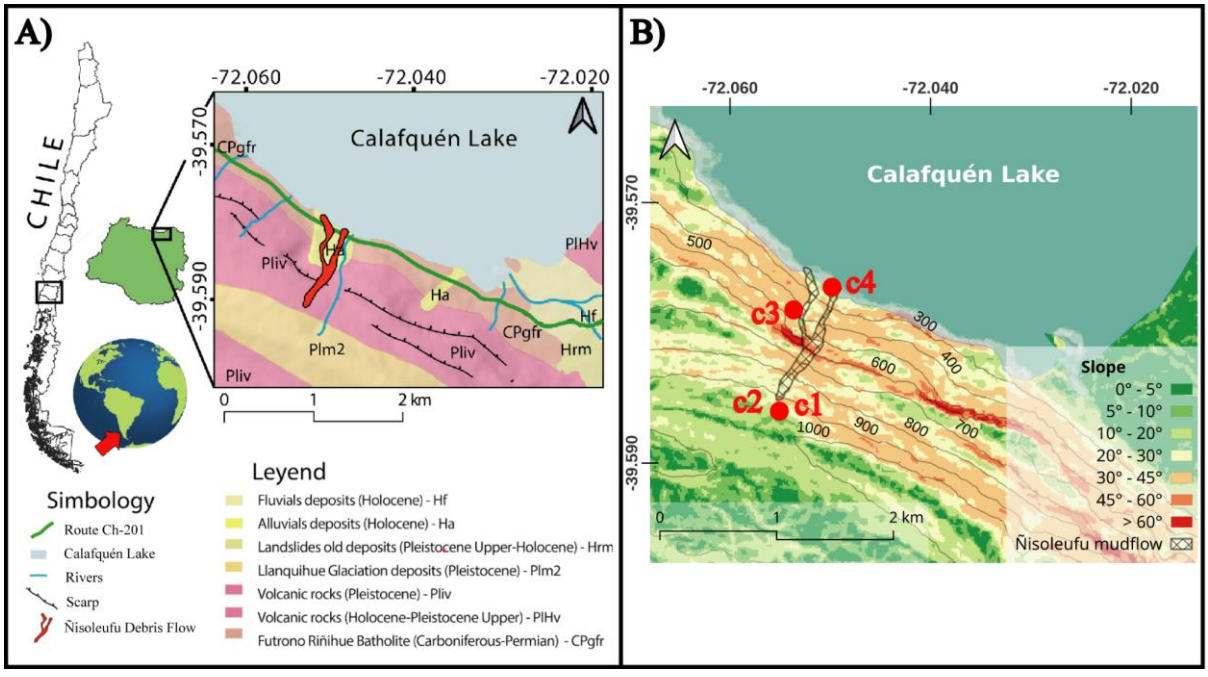

Figure 1 A) geological map of area study based on Rodriguez et al. (1999). B) slope and elevation values (m.a.s.l.).

The Ñisoleufu area exhibits a geological sequence **(Figure 1A)** starting at the base with the Futrono-Riñihue Batholith (CPgfr), followed by stratified volcano-sedimentary units (Pliv) and topped by glacial deposits (Plm2). Within this sequence, the Sierra Quinchilca volcano-sedimentary unit has been dated to less than 1 million years and is in nonconformity contact with the underlying rocks of the Futrono-Riñihue Batholith. Consolidated glacial deposits from the last glacial maximum period show variable depths, ranging from 1 metre to 10 centimetres, and lie in erosive unconformity over the volcano-sedimentary units (Pliv). The area also exhibits mass movement deposits (Hrm and Ha) covering the older units on the north slope of Sierra Quinchilca (Pliv, Figure 1**A;** Rodríguez et al., 1999).

3 Methodology

To assessed the triggering and conditioning factors in glaciar environments in Southern Andes, we assessed in detail the Ñisoleufu debris flow (Figure 2). To achieve this, we employed three complementary methodologies. The first methodology involved fieldwork, including soil sampling and subsequent laboratory analysis to evaluate the geotechnical features influencing debris flow initiation. The second methodology utilized numerical models to analyze meteorological conditions in the study area, such as precipitation patterns, variations in soil moisture, and landforms associated with erosion and deposition zones linked to the landslide. This endeavor involved a meticulous examination of the rheological and hydraulic attributes of the soil, facilitating an understanding of past and contemporary surface processes. Through this analytical framework, it

https://doi.org/10.5194/egusphere-2025-1394
Preprint. Discussion started: 9 April 2025

110 became feasible to discern causative factors contributing to the event, thereby enabling an informed evaluation of the potential risk posed by analogous occurrences in the future.

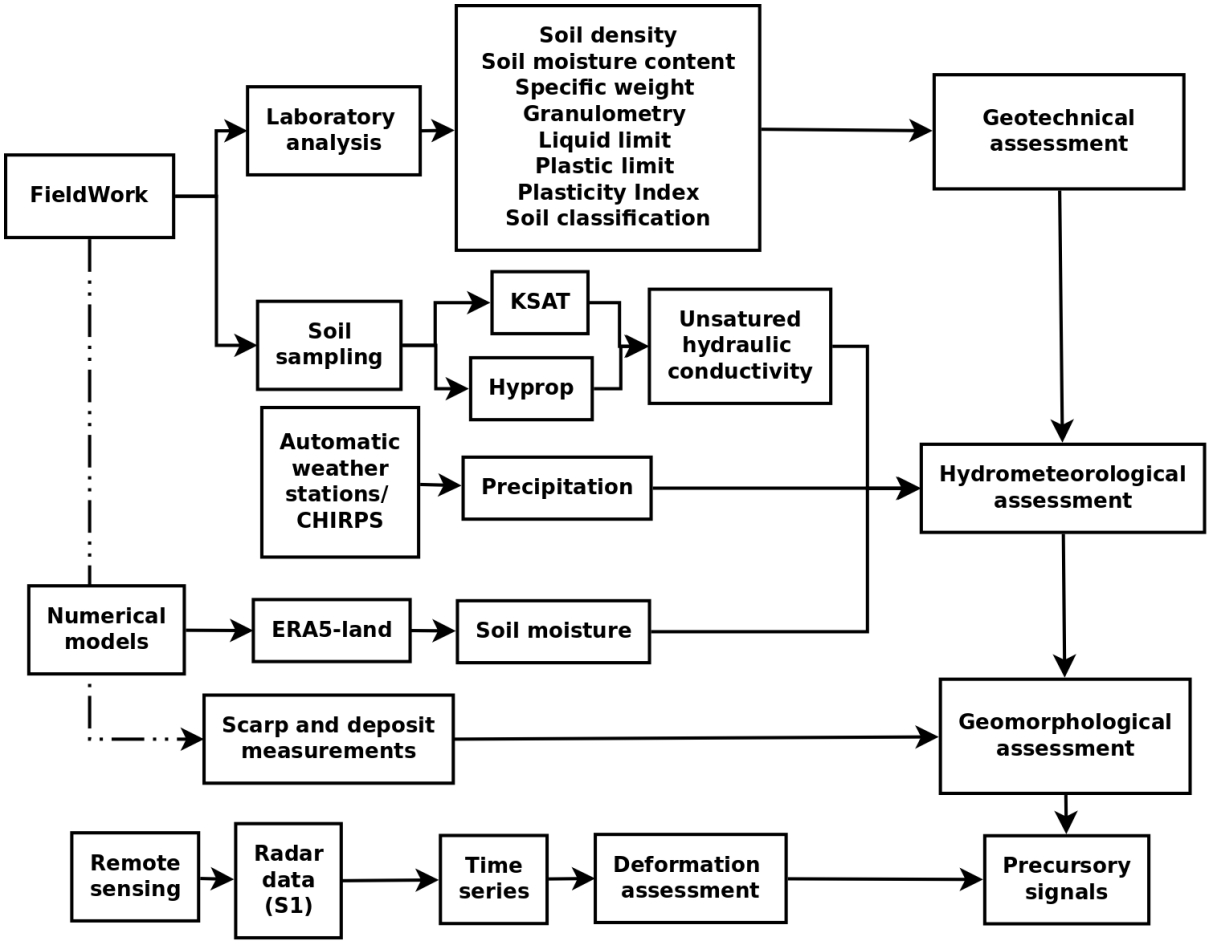

Figure 2 Methodological approach

115 **3.1 Geomorphological and geotechnical**

To analyse the geomorphological characteristics of the area, we utilised a 12.5 m resolution ALOS PALSAR DEM data, from which slope, aspect, and elevation maps were derived. A terrestrial and remote sensing survey was carried out to characterise the physiography of the hillslope before and after the debris flow. We employed the Normalized Difference Vegetation Index
120 (NDVI) to delineate the area affected by the debris flow. We calculated the NDVI using two Sentinel-2 acquisitions on May 13th, 2021, and June 14th, 2021, corresponding to the Ñisoleufu debris-flow event on May 31st, 2021. Field campaigns were conducted one day and three months after the event (June 1st, 2021 and September 2021) to characterise post-event

https://doi.org/10.5194/egusphere-2025-1394
Preprint. Discussion started: 9 April 2025

geomorphological features. Field observations were determinant in the identification of the sediment budget of the channel, aiding the assessment of the event's characteristics (a channelised, stony debris flow) and the movement dynamics in the hillslope. On-channel deposits were assessed using cross-sections along the Ñisoleufu sector. Peak flow marks were documented, and erosion depths were estimated based on erosion marks and bedrock exposures over three cross-sections.

Moreover, an exhaustive analysis of the geomorphological changes resulting from the event was conducted. A detailed survey of the stratigraphic column was conducted at three key points **(**Points c1, c2 and c4 in Figure 1**B)**. Firstly, a stratigraphy sequence at the base of the debris flow was generated, obtaining the deposit sequence and assessing previous non-documented events. Secondly, a survey was conducted in the headscarp area where the event was initiated, evaluating the geological and geomorphological conditions that led to its generation. This approach allowed for the characterisation of the strata and structures in the affected area, seeking insights into the triggering mechanisms of the flow. Additionally, a detailed evaluation of the lateral erosion caused by the flow was carried out to understand the impact of local geomorphological changes as proxies for similar glacial-volcanic environments (Bucher et al., 2024). Finally, the changes in vegetation that occurred as a consequence of the event (Figure 1B), allowing for the inference of the evolution of the post-event landscape and its influence on local eco-geomorphological processes.

To analyse the geotecnical features that support a debris flow generation or another type of mass wasting antecedent, soil samples were collected in the generation zone. We determined soil density (ρ) following the UNE 103-301-94, soil moisture content (NCh 1515), specific weight (ASTM D854-14) standards. Granulometry analysis was carried out using sieve and hydrometer methods based on Kinde et al. (2024). The liquid limit was determined using AS 1289.3.9.1, and the plastic limit was evaluated following NCh 1517/2 standard, allowing to obtain the Plasticity Index. Finally, the soils were classified based on ASTM D2487-17. These comprehensive geotechnical analyses provided crucial insights into the soil properties and their potential role in the occurrence of the debris flow event.

3.2 Hydrometeorological conditions

To analyse the hydrometeorological conditions, we investigate the influence of rainfall in the study area, analysing hourly/daily data from four weather stations from the INIA agrometeorological network (https://agrometeorologia.cl/) and the Climate Hazards Group InfraRed Precipitation with Station (CHIRPS) precipitation estimates (Funk et al., 2015). Soil moisture data from the ERA5-land product was utilised to complement the analysis considering the antecedent soil moisture at different depths before debris flow studies (Bordoni et al., 2023; Palazzolo et al., 2023), being considered suitable due to their accurate soil moisture data in hydrological studies (Muñoz-Sabater et al., 2021). The ERA5 product provides valuable and reliable information on soil moisture, enabling a more comprehensive understanding of the hydrological conditions that could trigger debris flows in the area. To understand the water transfer capacity along the soil, we measured the layer thicknesses from visual assessment of the soil profile in the scar **(**Figure 3**)**. We followed the experimental design of De Pue et al., (2019) considering two samples per layer. One sample was used to measure the soil moisture

https://doi.org/10.5194/egusphere-2025-1394
Preprint. Discussion started: 9 April 2025

(Θ (h)) and unsaturated hydraulic conductivity (K_u) using the evaporation method (HYPROP®, Meter Group), meanwhile, saturated hydraulic conductivity K_s was measured using KSAT® equipment (Meter Group), using the falling head method **(Dane et al., 2002).** The hydraulic conductivity will provide valuable information about the layer's ability to allow water to flow through, which could have played a significant role in the initiation and propagation of the debris flow.

3.3 Remote sensing and precursory signals

We assessed precursory signals estimating surface deformation by the Stanford Method for Persistent Scatterers (StaMPS) using Sentinel-1 C-band SAR data. We downloaded 35 ascending orbit (track 164) and 18 descending orbit (track 83) Sentinel-1 images covering the period from November 2020 to June 2021, which includes seven months before the May 31st debris flow in the Ñisoleufu sector (Table 1). We also included two acquisitions after the debris flow in both orbits to analyse the slope's response to non-rainfall and rainfall periods. Initially, we analysed data until the end of July, but snow coverage led to coherence loss in the area, resulting in a low density of Persistent Scatterer points (PS points) per km^2. Consequently, we evaluated different combinations of bands from Sentinel-2 images (based on bands 4, 3, 2) to assess the maximum amount of SAR images available before the snow period. This approach allowed us to optimise the data selection process and continue our analysis effectively.

The SAR data was processed using open-source Sentinel Application Platform (SNAP) packages through the snap2stamps routines, enabling us to generate single-master interferograms compatible with StaMPS. Further details on the snap2stamps routine in Foumelis et al. (2018) and Blasco et al. (2018). First, the initial selection of PS points is performed based on their noise characteristics, using the amplitude dispersion criterion, which is defined by $D_{Amp} = \sigma_{Amp}/m_{Amp}$, where σ_{Amp} and m_{Amp} are the standard deviation and mean of the amplitude in time, respectively (Ferretti et al., 2001). We selected a threshold value of 0.4 for D_{Amp} as a typical threshold value (Hooper et al., 2007), and subsequently, some initial parameters were modified according to the values proposed by Höser (2018). This allowed us to plot surface soil deformation using time series, which we then compared with daily precipitation records obtained from nearby weather stations and satellite measurements. Lastly, we used the GACOS correction (Yu et al., 2018) through the TRAIN toolbox (Bekaert et al., 2015) to reduce the atmospherical phase component. We complemented surface deformation with antecedent precipitation to establish precursory signals and their correlation with precipitation. We calculated the accumulated precipitation between the dates of the SAR acquisitions and the total accumulated precipitation for the entire period. We assessed daily precipitation and their temporal changes to understand the antecedent precipitation in the debris flow event. We specifically selected data from the Pucón station and CHIRPS dataset for comparison with the time series of deformation to examine the relationship between precipitation and deformation.

Table 1 Data used in temporal analysis using SAR data.

https://doi.org/10.5194/egusphere-2025-1394
Preprint. Discussion started: 9 April 2025

	Track	Frame	First Image	Last Image	Total Images	Primary Image	Sub-Swath
DES	83	93	02 November 2020	18 June 2021	18	02 March 2021	IW2
ASC	164	1048	01 November 2020	17 June 2021	35	11 February 2021	IW3

4 Results

4.1 Geomorphological and geotechnical conditions

The extension of the area affected by the debris flow was evaluated, identifying and characterizing the triggering conditions (Figure 4**A).** The results revealed significant differences in the Normalized Difference Vegetation Index (NDVI), which facilitated the delimitation of the landslide area **(**Figure 4**A)**. Low positive NDVI values (<0.20) are shown for the area affected by the debris flow, encompassing 118,575 m², in contrast to the normally high NDVI values (0.6-0.8) of surrounding areas. The debris flow moved along a complex and abrupt geometry, with slopes varying from 20° near the ridges (950 m a.s.l.) and the base of the slope (250 m a.s.l.), to almost vertical areas (~90°) in the intermediate zone (550 m a.s.l.) **(**Figure 3**A and** Figure 4**D)**. This geomorphological configuration is typical of glacially eroded valleys (U-shaped valleys) in the southern Andes, a recurrent phenomenon in the formation of valleys at this latitude(Muratli et al., 2010).

The initial landslide crown has an altitude of 950 m a.s.l. and slopes of approximately 20 to 30° (column c1 in Figure 3**B**). The flow release zone (inset C in Figure 3) has evidence of extensional failures, where c1 indicates that the first level S-1 corresponds to a very compact chaotic and polymictic till deposit (Plm2), with a greyish matrix containing a higher percentage of clay than sand. Some clasts exceed 10 cm and are composed of volcanic fragments (Pliv), as well as intrusive material (CPfgr). Towards the top of the glacial deposit, level S-2 is observed, a thin, grey fluvioglacial deposit (varves), approximately 40 cm thick, composed of a well-consolidated matrix of clay-rich (dark) and silt-rich (light) setting a couplet annual sediment layer. **(**Figure 3**C,** Figure 3**D and** Figure 4**D)**. Above the glacial deposit, level S-4 is identified, composed mainly of lapilli-sized deposits (>5 mm), associated with pumice from the Neltume deposit of the Mocho-Choshuenco Volcanic Complex, dating 10,200+-500 BP (Rawson et al., 2015; Moreno-Yaeger et al., 2024). Finally, level S-7 corresponds to the current soil where native forest develops (Figure 3**B**).

https://doi.org/10.5194/egusphere-2025-1394
Preprint. Discussion started: 9 April 2025

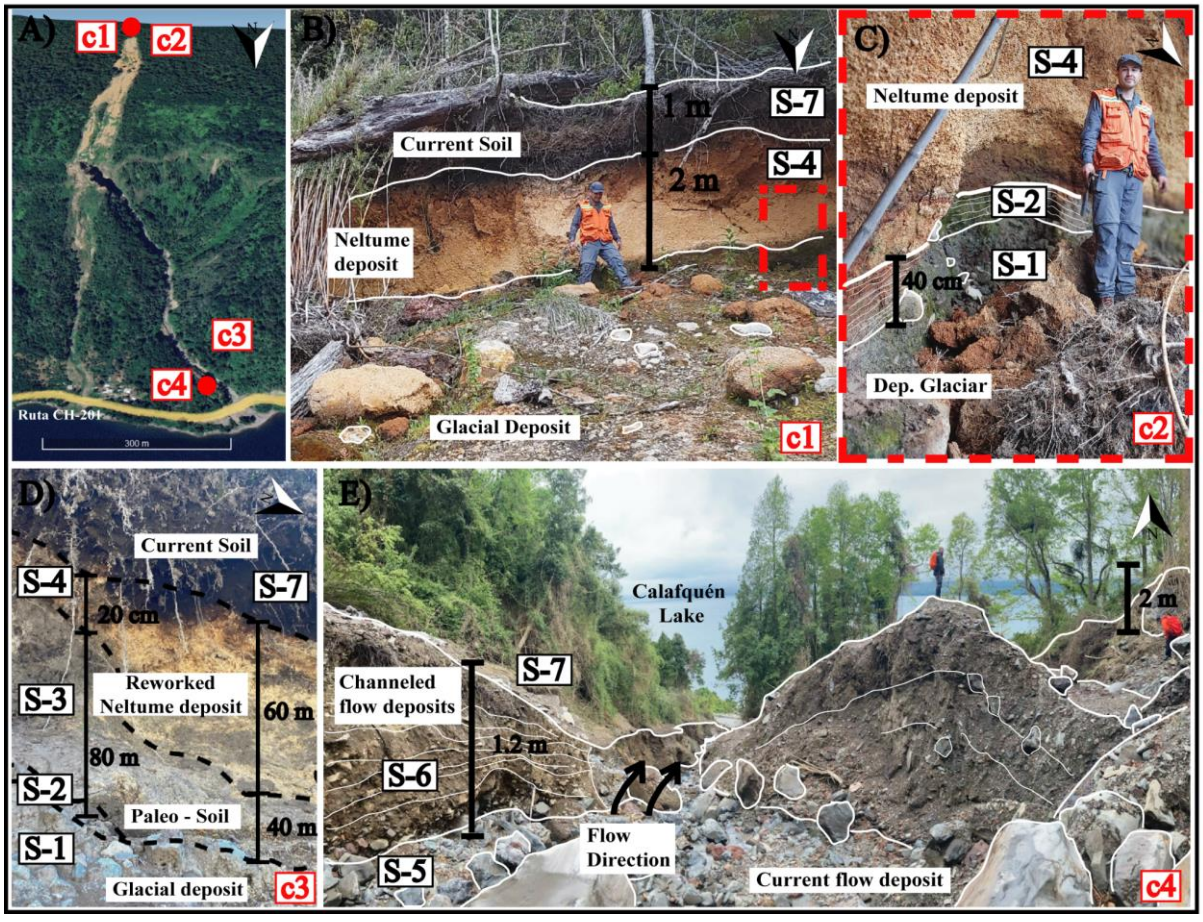

Figure 3 Field photographs indicating soil deposits in scarp (B and C) and the deposits in the toe (inset D and E).

In relation to the channelled flow deposits, the blocks and gravels are predominantly (~75%) composed of material from Sierra Quinchilca, while a smaller proportion (~25%) is composed of granodiorite from the Futrono-Riñihue Batholith (Figure 4**D**). The composition of the matrix deposit is derived from the slope volcanic and glacial deposits (Rodríguez et al., 1999). This geological and soil composition is representative of a typical distribution in the Southern Andes, specifically spanning the latitudinal range from 39° to 42°S.

Below the steepest slope zone of the hillslope, sequences with significant spatial variability were identified (Figure 4B-D). At 350 m a.s.l. (column C3) slopes vary between 30 up to 45°. The basement associated with the CPfgr crops out at the base, in erosive contact with level S-1, mainly related to glacial deposits with the presence of large angular blocks. Laminar levels of clay and silt towards the top (S-2) stand out. Above the glacial deposit is level S-3. At first glance, the paleosol observed in c2 appears to have a relative age younger than the glacial deposits but older than the Neltume ashfall deposit. However, field observations indicate that paleosol S-3 is younger than the Neltume ashfall, as level S-4 in c3 represents a reworked deposit

https://doi.org/10.5194/egusphere-2025-1394
Preprint. Discussion started: 9 April 2025

derived from this ashfall event (S-4). The presence of imbricated pyroclasts and their noticeable variation in thickness (Figure 3D) support this interpretation. Finally, at the top of the sequence illustrated in columns c3 and c4, level S-7 shows active soil development, reaching approximately half of the thickness observed in column c1.

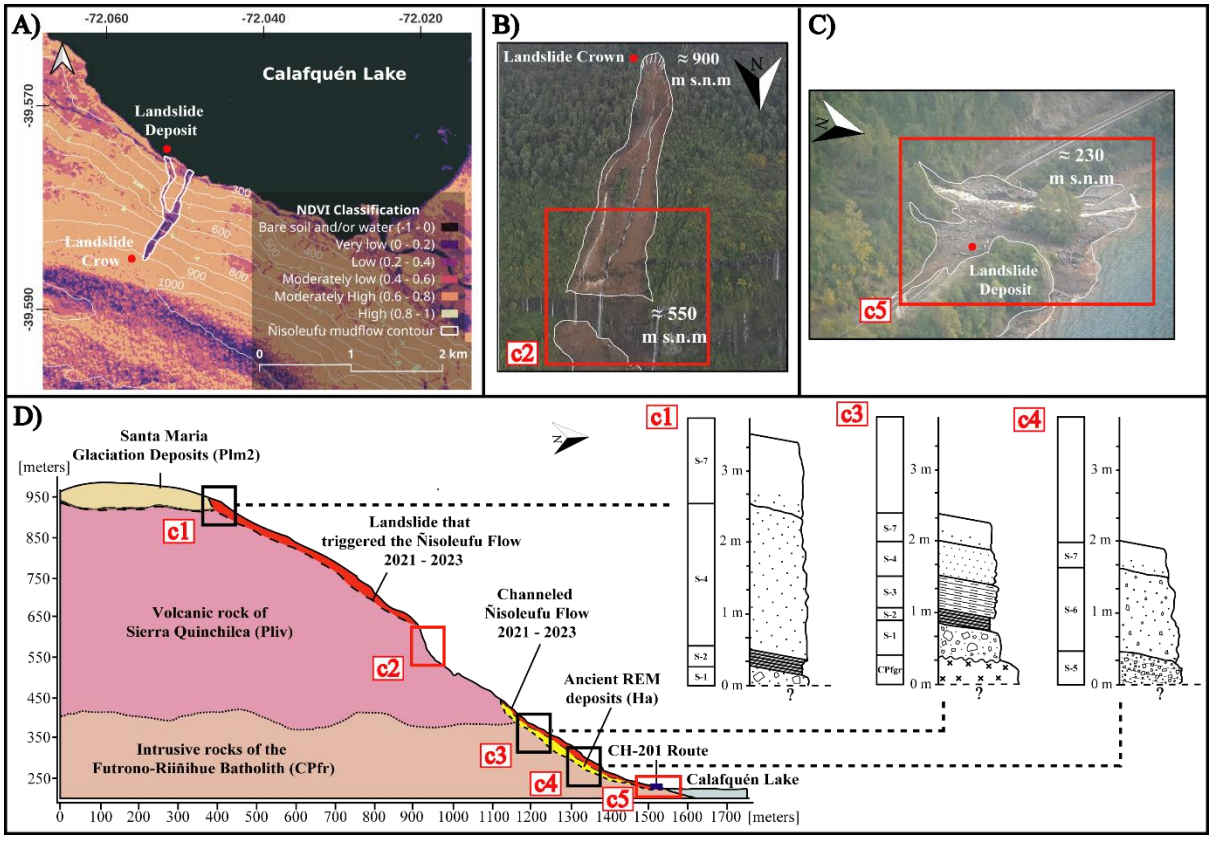

Figure 4 A) Normalized Difference Vegetation Index (NDVI) highlighting the erosive zone generated by the Ñisoleufu debris flow. B) and C): Photos taken by a drone on 01 June 2021, highlighting the crown of the debris-flow (B), and the landslide deposit and the development of many waterfalls around the flow in red (C). D) Profile of the sequence where the flow occurred and stratigraphic columns. Photos: Carrasco and Ramirez (2021).

Near the base of the flow, at an altitude of 250 m a.s.l. and with slopes between 0 and 20°, a sequence without the levels observed in the previous points upstream was identified **(**Figure 4**)**. The area represented by column **c4**, showed soil levels associated with previous mass wasting events **(**Figure 3**E)**. At the base, level S-5 is identified, associated with a polymictic deposit with a high presence of clasts, reaching a size up to 10 cm, and slight northern imbrication. The matrix of the deposit has pumice content from the Neltume deposit (S-4), related to the explosive event of the Mocho-Choshuenco volcanic complex, and clays from the glacial deposits (S-1 and S-2), present upstream as observed in columns c1 and c3. Above the flow is another level (S-6) with the same characteristics, but with a lower proportion of clasts with respect to the matrix. Finally, towards the top, the development of the current soil (S-7) is observed, with a thickness like that measured in column c3.

https://doi.org/10.5194/egusphere-2025-1394
Preprint. Discussion started: 9 April 2025

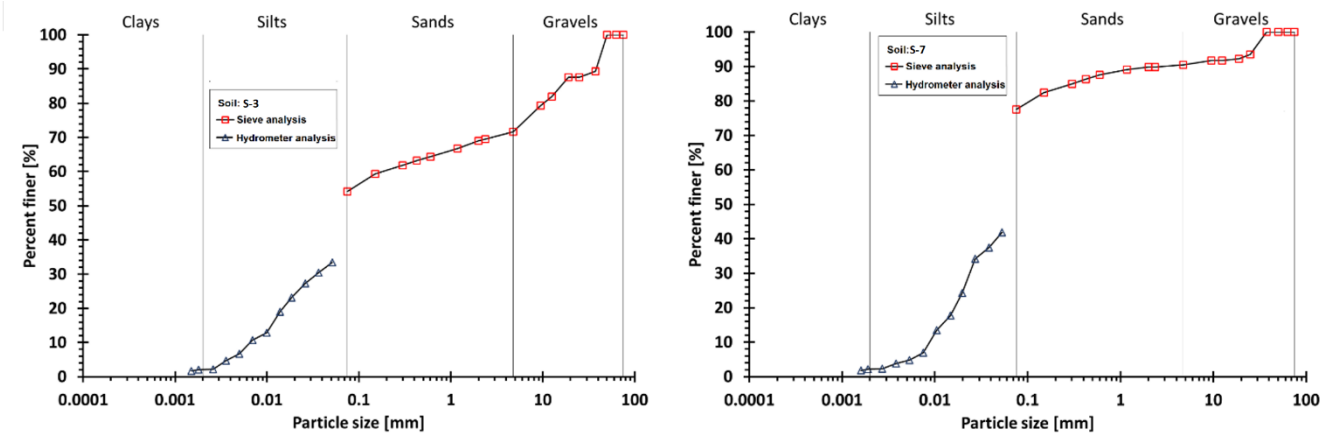

240 **Figure 5 Soil granulometric curve of S-3 and S-7.**

Table 2 Physical properties of soils related to the column C3.

Soil type/Property	Normative	S-2	S-3	S-4	S-7
Moisture [w%]	NCh-1515	17.8	56.2	119.3	111.6
Density [ρ] (gr/cm3)	UNE-103-301-94	2.07	1.52	<1	1.06
Specific Gravity [Gs]	ASTM-D854-14	2.76	2.49	2.5	2.34
Liquid Limit [WL] (%)	AS 1289.3.9.1	27.48	123.93	-	149.83
Plastic Limit [WP] (%)	Nch 1517/2	16.07	91.3	-	114.13
Plasticity Index [PL]	NCh1517/2	11	33	-	36
Hydraulic Conductivity [ku] (m/s)	Porchet and Laferrere (1935)	-	-	-	3.13E-4

245 From a geotechnical perspective, the first soil (S-2) has a liquid limit of 27.48 and a plastic limit of 16.07, resulting in a plasticity index of 11. This soil exhibits a low plasticity and is classified as a silt (CL) according to the Unified Soil Classification System (USCS). S-3 showed a liquid limit of 123.93 and a plastic limit of 91.3, resulting in a plasticity index of 33. This soil exhibits a moderate plasticity and is classified as a plastic silt (CH), according to the USCS. Meanwhile, S-7 has a liquid limit of 149.83 and a plastic limit of 114.13, resulting in a plasticity index of 36, showing a high plasticity and is
250 classified as a plastic organic soil (OH). The granulometric analysis (**Figure 5;** S-3 and S-7) confirms this classification, with silt and sand content between 70% and 90%. Due to the soil properties, S-4 (Neltume ashfall pyroclastic) has not been characterised in the laboratory due to the high fragility of the pyroclasts classified as lapilli (Ø>5 mm) being too coarse to measure their limits.

https://doi.org/10.5194/egusphere-2025-1394
Preprint. Discussion started: 9 April 2025

4.2 Hydrometeorological conditions and precursory signals

The debris flow release zone (column c1 in Figure 3**B and** Figure 4**B**) provided accurate soil measurements using KSAT, enabling us to understand the factors governing water transport on the slope. Field mapping revealed a layered model that identified a highly stratified environment with distinct characteristics (Figure 3**C**; Table 3). It was observed that the glacial deposits underlying layers of volcanic origin regulate water movement in the soil due to their low hydraulic conductivity (Table 3). These glacial deposits, identified as moraines and varves, are associated with the Last Glacial Maximum (LGM), correlated with nearby deposits and natural terrain conditions.

Notably, volcanic soil deposits (**Figure 5**; granular texture description) and Neltume ashfall demonstrating high saturated hydraulic conductivity of 4.64E-5 to 3.31E-04 m/s (Table 3). This characteristic is critical as it facilitates the movement of infiltrated water from the organic surface to the slope's interior. In contrast, Varves-type glacial deposits show low hydraulic conductivity, with values of 1.54E-05 m/s, while the till reached a Ks of 2.65E-05 m/s, both acting as partial barriers to water movement. Nevertheless, their storage capacity is significant, particularly when situated on moraines that, due to their varied granulometric distribution, retain water effectively. The hydraulic conductivity and the high infiltration rated derived from the Porchet test showed a moderately high infiltrated rate (112.70 mm/hr), computing a k=3.31E-4 (m/s) in the superior organic deposit layer (S-7; Table 2 **and** Table 3).

Table 3 Hydraulic properties of release zone in debris flow generation zone (column c1 in Figure 1).

Layer	depth (m)	Ks @10C (m/s)	Description
Superior layer	0-0.5	3.31E-04	Organic (S-7)
Volcanic deposit 1	0.5-2.5	2.24E-04	Neltume ashfall deposit (S-4)
Volcanic deposit 2	2.5-2.7	4.64E-05	base Neltume (S-4)
Varve	2.7-3.0	1.54E-05	Varves (S-2)
Morraine	3.0-??	2.65E-05	Saturated Morraine (S-1)

Analysis using the ERA5 model reveals a pronounced annual cycle in soil moisture (Figure 6). Antecedent precipitation data indicated a surface saturation, showing a shallow condition reaching a full saturation in the first metre of depth, mainly related to previous rainfall events (Figure 6**B-C**). Moreover, a substantial increase in soil moisture was identified at greater depths (up

https://doi.org/10.5194/egusphere-2025-1394
Preprint. Discussion started: 9 April 2025

to 2.89 meters), exhibiting a rapid 50% change preceding the onset of flow events (Figure 6**B**). This notable fluctuation in soil moisture occurred specifically at the interface between tephra and till-varves, implying potential implications for the natural stability of the terrain base.

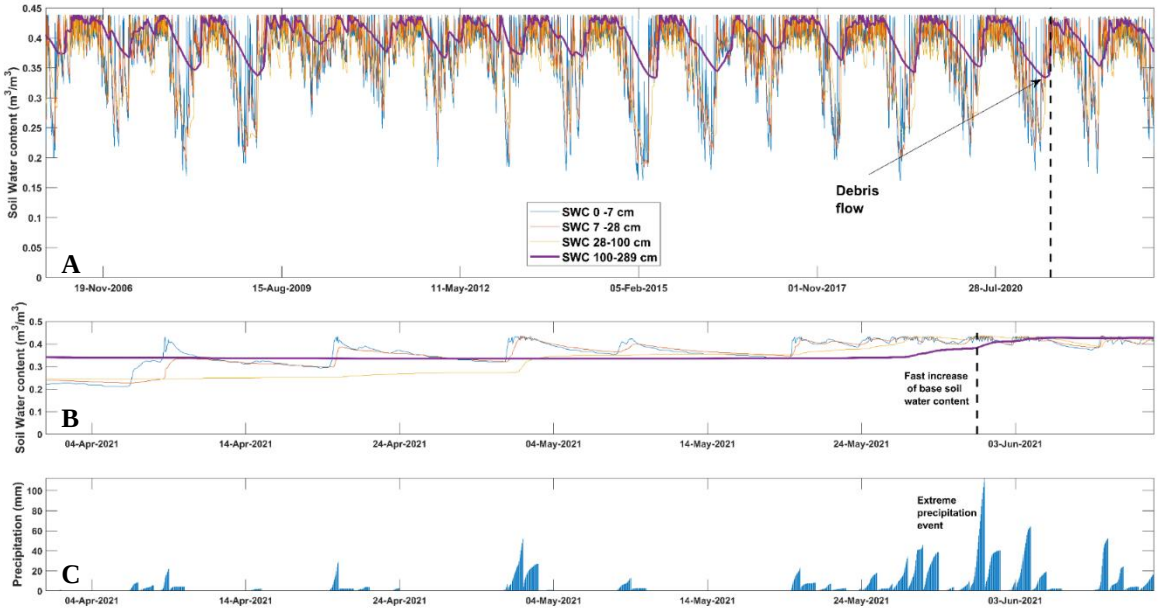

Figure 6 Assessment of ERA5-land product over debris flow generation. A: Assessment of time series of soil moisture at different depths. B: Zoom to Soil moisture weeks previous to debris flow. C: Rainfall events accumulated at 24-hourly scale (ERA5-land).

The availability of a sufficient quantity of SAR images and the revisit times of Sentinel-1 enabled a well-distributed temporal analysis of slope behaviour before the debris-flow event on May 31, 2021. We measured surface deformation between -1 and -32 mm/year. The results of PS estimation suggest the occurrence of surface subsidence consistent change in soil water content (Figure 6B). Our results suggest a precursory deformation signal based on two distinct periods (Figure 7)**.** The first period displayed a consistent deformation pattern extending from December 2020 to the end of March 2021, characterized by precipitation concentrated mainly in three intervals (mid-December, late January, and mid-March; Figure 7). These precipitation events infiltrated into the soil, leading to increased soil moisture (Figure 6A). A second period (accelerated deformation) was characterized by pre-event deformation patterns following a high precipitation event in May 2021. Our results suggest that the variation in surface deformation rates could be a response to a significant precipitation event that occurred at the end of January, being related to the high-intensity rainfall throughout the second half of May (Figure 7). This temporal relationship between precipitation and deformation further underscores the need for incorporating hydrological factors into models of surface stability and landslide risk assessment.

https://doi.org/10.5194/egusphere-2025-1394
Preprint. Discussion started: 9 April 2025

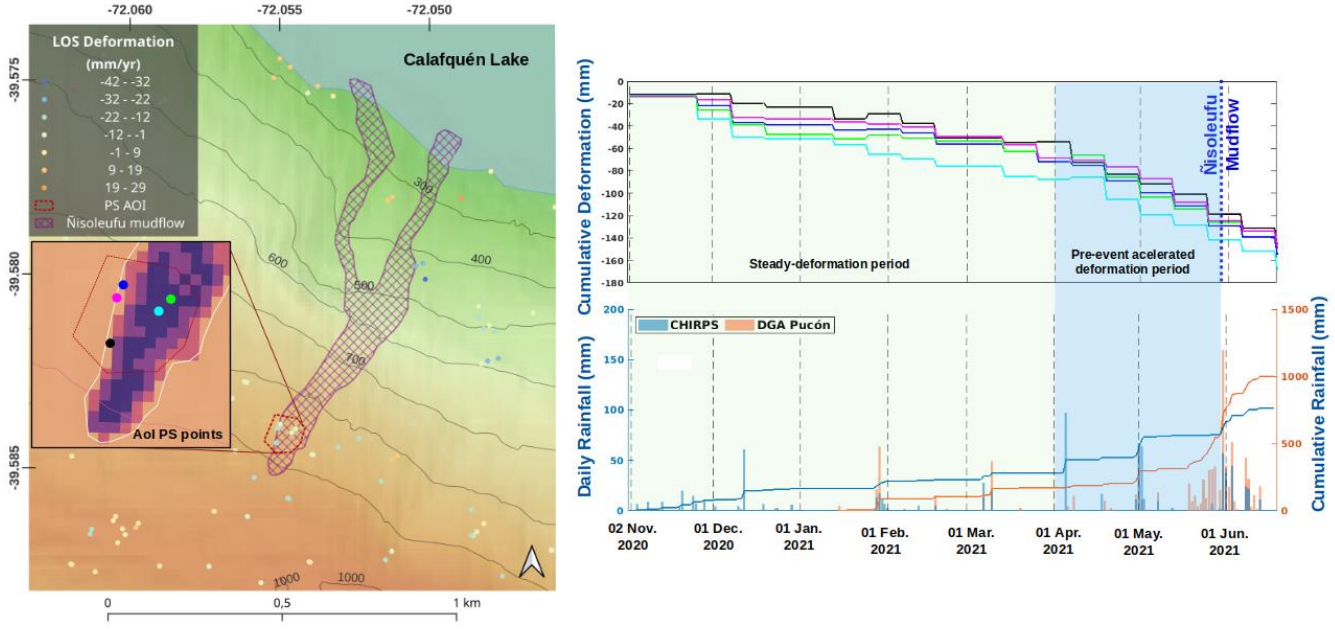

295 **Figure 7.** Left panel: PS points obtained with Sentinel-1 "descending" orbit data. The colors of the gray panel located in the upper left (warm tones [red] to cool tones [blue]) represent the LOS deformation (PS in mm/yr). According to the colors distributed in the main image, deformations range from -1 to -32 mm/yr. The zoom on the debris flow head shows representative PS points for the area. However, in this zoom, each PS point was assigned a new pattern color in order to clearly identify each deformation trajectory over time, plotted in the right panel. Right panel up: Cumulative deformation time-series obtained with Sentinel-1 descending orbit data related to PS points. Right panel
300 down: precipitation time series using CHIRPS satellite estimates (blue) and data records from INIA meteorological stations (orange, Pucón station).

5 Discussion

We studied the conditioning and triggering conditions of debris flow in an area to understand precursory signals of mass wasting initiation in post glacial and volcanic environments. We considered a geomorphological, geotechnical,
305 hydrometeorological and surface deformation approach to constraint the variability of the mass wasting processes in one representative area of the Southern Andes.

5.1 Geomorphological and geotechnical implications

The occurrence of mass wasting events, such as landslides and debris flows, following periods of intense rainfall has been extensively studied in the Southern Andes using local cases, mainly based on the rainfall control over the mass wasting
310 generation (Fustos et al., 2020; Maragaño et al., 2023) without consider the soil features as noted in recent studies (Vasquez-Antipan et al., 2025). Our results showed that the geomorphology plays a crucial role in the generation of debris flows,

https://doi.org/10.5194/egusphere-2025-1394
Preprint. Discussion started: 9 April 2025

particularly through its influence on water accumulation in catchment areas, such as micro-basins (Fustos-Toribio et al., 2021). We considered two main geomorphological controls for debris flow initiation. First, stand out the steep slope (>45°), which was a significant contributing factor to the generation of the Ñisoleufu debris flow (Figure 1 **and** Figure 4**B-D**). Second, the northern orientation of the slope could also be a relevant factor, as in the central-southern Chile domain (36°-42°S), atmospheric moist flux from extreme rainfall tends to flow in a northwest (NW) direction, with orographic forcing triggering being enhanced by the Andean belt (Valenzuela and Garreaud, 2019; Vasquez-Antipan et al., 2025). The interplay between areas with high water accumulation capacity from local runoff and the slope's propensity to capture precipitation was instrumental in the generation of the debris flow. Stand out the slope that facilitated an efficient surface drainage of water from higher areas, leading to the formation of local accumulation and infiltration zones that promote the build-up of subsurface pore-water pressures (Table 3) leading to the debris flow event, facilitating a rapid downslope movement of soil once it became saturated.

The geotechnical stability of soils in the Southern Andes, could be controlled by the interaction between explosive volcanic. Mocho-Choshuenco volcanic complex (MCVC) and glacial processes and the resultant varved deposits (Figure 4) has been modulated the slope stability around the 39°S. The Neltume ashfall deposit related to the eruption of the MCVC (10,200+-500 BP; Rawson et al., 2015) played a significant role in the formation of the S-4 (Figure 3**B-C**). The thickness of all soils varies along the scar left by the debris flow, with the magnitude strongly influenced by the topographic gradient and/or erosion processes that might have occurred and following reworking (Figure 3D). Moreover, glacial deposit like as varves, formed from sedimentation during glacial periods, played a crucial role in the soil's physical and mechanical properties controlling the area with low hydraulic conductivity (Table 3) introducing a water barrier in the area to regional scale.

Moreover, field evidence suggests that the Ñisoleufu event is not an isolated case as seen in the removilized events (Figure 1, geological map - alluvial deposit: Ha). The geotechnical properties of the material to be remobilized are crucial for establishing stability conditions. The granulometric characteristics of the deposits, primarily granular types associated with S-4, are identified as frictional soils overlying fine-grained, cohesive soils like varves (S-2). Other soils in Southern Andes, such as S-3 and S-7, could be originated from the decomposition of volcanic glass from ashes and glacial clays (Sanhueza et al., 2011), resulting in particles smaller than 0.1 mm (Figure 5). The distribution of the soil layers varies abruptly downslope, as observed with S-1, S-2, and S-4 in columns c1 and c3, showing and intense mass wasting and erosion productivity in areas close to glacial lakes (Figure 4D). The frictional soils, related to S-4, exhibit high shear resistance (Chen et al, 2021) combined with steep slopes can contribute to stability control of post-glacial volcanic deposits (Walding et al, 2023; Ontiveros-Ortega et al, 2023). However, while frictional soils are generally more resistant to sliding (Chen et al, 2021), soil saturation can significantly decrease their strength, thus increasing the risk of failure under extreme precipitation events detected in recent years in the Southern Andes (Somos-Valenzuela et al., 2020; Fustos et al., 2021). This is consistent with the presence of extensional failure observed before flow initiation and subsequent reactivations on June 2023 and 2024 (Figure 3C; Figure 8).

https://doi.org/10.5194/egusphere-2025-1394
Preprint. Discussion started: 9 April 2025

We propose that the event of Ñisoleufu, a classical case of the Southern Andes, was triggered by the soil saturation, reducing the effective stress within the soil matrix leading to extensional failure in the volcanic deposits (Figure 3B; 8). Recent studies have highlighted the risks associated with this saturation, particularly in areas where explosive volcanic activity has previously occurred, leading to increased susceptibility to debris flows and other forms of mass wasting (Pola et al., 2020). The interaction between glacial deposits and volcanic materials creates a unique geotechnical environment where the stability of slopes is contingent upon both the physical properties of the soil and the hydrological conditions present (Pisabarro & Cañadas, 2020).

5.2 Hydrometeorological conditions and precursory signals implications

The volcanic origin and composition of the soils evidenced a high soil moisture variability along the year. ERA5-land data reveals a sudden change in soil moisture content at various depths on the base of the debris flow initiation supporting the surface deformation days before the landslide (Figure 7). The water role in the event propose that accumulation of subsurface water in granular soil could serve as a storage medium. The fine media of S-1 and S-2, with its low hydraulic conductivity, acts as barrier layer, enhancing the storage capacity of S-4 in the crown of the debris flow. This is supported by the hydraulic properties of S-3 (CH) and S-7 (OH), combined with Porchet's study on the current soil (S-7: 112.70 mm/hr), which indicates a moderately high infiltration rate and suggests high hydraulic conductivity for the Ñisolelfu soils (Table 3). The combination of these factors contributes to the overall permeability of the volcanic soils, main feature in the Southern Andes, potentially influencing water movement and retention in the area.

The water storage is consistent with surface accumulative deformation data, reaching -50 mm in the previous 60 days of the event (accelerated deformation period), offering insights of previous surface deformation to the occurrence of debris flow events in areas where glacial deposits and volcanic deposits coexists. The atypical nature of these deformations suggests that the surface experienced slow movements associated with subsidence along the LOS direction, preceding the debris-flow event on May 31, 2021. This event coincided with significant rainfall recorded at the Pucón station (159.8 mm/24 hrs). The constant slope deformation support the hypothesis of the development of extensional failure, ultimately resulting in the observed a landslide and subsequent release of water as debris flows (inset C in Figure 3**;** Figure 8).

The fast saturation of S-4 is exacerbated by increased water availability due to rainfall and by the presence of a bottom layer with low hydraulic conductivity associated with fine soils (S-2), being a common denominator in the Southern Andes. S-2 retains water and further reduces the shear strength of the underlying granular soil. Additionally, these soils could act as lubricants, reducing the overall slope shear strength. The interaction between glacial deposits and explosive volcanic eruption deposits in the cordilleran zone of the Southern Andes creates a scenario prone to slope deformation and mass removal, especially debris flow. Our results suggest that the combination of geological and climatic factors in this region generates ideal conditions for the occurrence of mass removal events under extreme precipitation events.

https://doi.org/10.5194/egusphere-2025-1394
Preprint. Discussion started: 9 April 2025

5.3 Regional implications and Future Scope

The Southern Volcanic Zone (37.5° - 41.5°S; Stern 2004) has been shaped by significant volcanic Holocene eruptions (Fontaine et al., 2021; Moreno-Yaeger et al., 2024; Singer et al., 2025), leading to the formation of soils primarily composed of lapilli and/or ashes that settled following the contours of the topography, resulting in layers with varying thicknesses (Stern, 2008). Old deposits in the zone show similarities to the current debris flow deposits (Figure 4**B**), suggesting that the event triggered in 2021 is not an isolated occurrence in the area. This evidence points to a history of recurring debris flow events in the region. This condition is dominant in all the surroundings of the Mocho-Choshuenco volcanic complex (Rawson et al., 2015; Moreno-Yaeger et al., 2024). The Ñisoleufu debris flow showed a characteristic pattern of mass wasting processes in the Southern Andes, becoming analogues to Petrohue event (Fustos-et al., 2021). Our results show that precursory signals such as small progressive deformation of the surface (Figure 7) could suggest the indication of possible soil slides previous to initiation of the debris flow (Figure 8). This phenomenon is influenced by fine soil interspersed with glacial deposits, superimposed on moraines and volcanic deposits, common throughout the southern Andean region (Moreno-Yaeger et al., 2024; Singer et al., 2024). A simple geomorphological generalization highlights the necessity of investigating the interaction

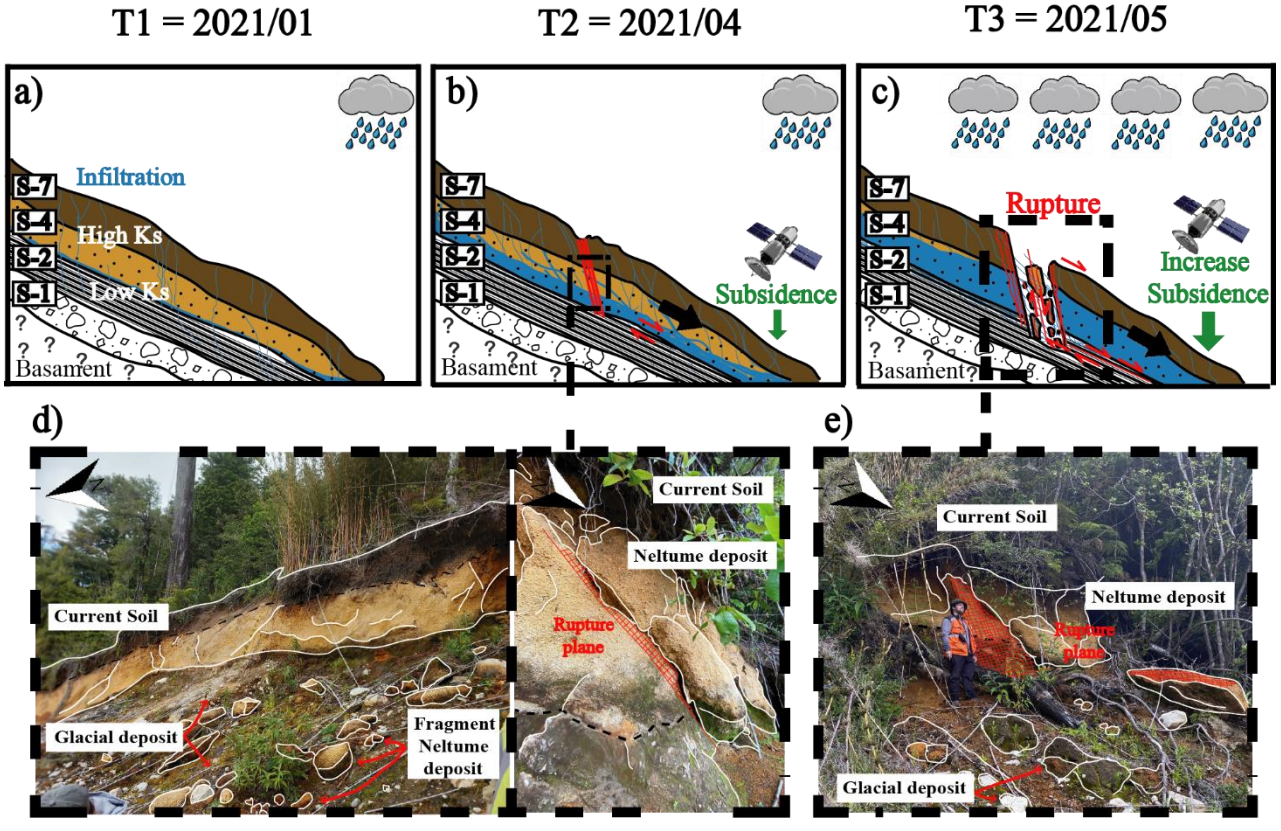

https://doi.org/10.5194/egusphere-2025-1394
Preprint. Discussion started: 9 April 2025

Figure 8 Conceptual model of soil deformation and following failure under cryospheric constraint. A) First phase with low precipitation. B) Start of the extensional failure and small-rate deformation measured by satellite. C) Failure and initiation of the landslide and following debris flow. D) Scarp in the crown with extensional signatures (white lines) E) First plane of the current rupture plane that could generate new debris mass wasting.

between glacial and volcanic deposits to understand better the interplay between media with constraints on soil hydraulic conductivity. Future studies should prioritise examining these dynamics to prevent and mitigate potential risks associated with similar landslide events across the broad area of the Southern Andes.

Debris flow generation in volcanic soils and their correlation with post-glacial eruptions, assumes a critical importance in comprehending the mass wasting hazards under the current climate crisis. Holocene eruptions, known for their Plinian events such as Mocho-Choshuenco, Carran-Los Venados, Calbuco, Chaiten in the Southern Andes (Singer et al., 2024), have yielded abundant tephra and volcanic soils possessing high hydraulic conductivity. These eruptions formed volcanic deposits over moraine and varve deposits (Figure 3). The volcanic soil acts as a high-rate infiltration layer meanwhile, the moraine crowned by impermeable varve layers in the base of the sequence plays a reservoir on (Figure 8). Therefore, the amalgamation of these deposits with intense precipitation events may expedite the loading of these reservoirs, heightening the probability of slope instability due to increased mechanical load and pore-stress changes (Bogaard & Greco, 2015). Early indications of this phenomenon are evident in occurrences such as Chocol (2023, and Volcán Osorno (every year), suggesting a potentially heightened recurrence in the future. To mitigate the associated risks effectively, it is imperative to enhance the zoning of areas prone to debris flows in the Southern Andes, thus minimizing the impact on population and infrastructure within these vulnerable zones.

Our study proposes considerations that must be assessed in landslide research in the Southern Andes, allowing a deep understanding of the interplay between geomorphological, geotechnics, hydrometeorological and remote sensing analysis, allowing a better landslide risk assessment and mitigation efforts in the region. We propose that the Ñisoleufu event could as study case for researchers and authorities can better comprehend the specific conditions that lead to debris-flow occurrences and implement appropriate measures to minimize the impact of such events in the future.

6 Conclusions

We studied the conditions that evolved in the generation of debris flows in the Southern Andes, an area modulated by the glacial and volcanic processes. The mass wasting could be influenced by complex interactions among geomorphological, geotechnical, and hydrometeorological factors (Figure 8). The geological environment of the Southern Andes, characterized by a mix of volcanic and glacial deposits, showcases unique soil properties affecting overall slope stability. The mechanisms leading to mass wasting, particularly the Ñisoleufu event, underscore the critical roles of soil saturation and effective stress reduction in triggering slope failures (Figure 6). The analysis of geomorphological factors revealed that slopes greater than 30 degrees significantly contribute to debris flow triggers, as supported by studies emphasizing rainfall's role in mass wasting (Figure 4). The orientation of these slopes, particularly aspects with more rainfall exposure, promotes precipitation

https://doi.org/10.5194/egusphere-2025-1394
Preprint. Discussion started: 9 April 2025

accumulation from extreme weather patterns. Our findings corroborate the influence of gradual accumulation of subsurface water, aided by low hydraulic conductivity from underlying soil layers (Table 3), can create critical saturation levels that reduce shear strength and lead to flow initiation. These processes, not considered in detail in previous studies, must be integrated in future assessment in detail into the future.

We conclude that recurrence of mass wasting is influenced by past volcanic eruptions and post-glacial conditions. A comprehensive understanding of the interplay between geological and hydrometeorological conditions is crucial for forecasting debris flow risks in the Southern Andes, particularly considering climate change, which may exacerbate extreme weather events. We highlight that while frictional soils can provide stability under dry conditions, they become increasingly vulnerable to failure under saturated conditions as was evidenced in the Ñisoleufu event. The data indicating surface deformation prior to debris flow events (Figure 7 and 8), demonstrating that precursory signals that can be leveraged for early warning systems. The velocity of surface movements preceding the Ñisoleufu event are correlated with increased soil moisture levels, emphasizing the utility of integrating remote sensing technologies to monitor these changes as proxy. Our findings could be extended to regional scale as conceptual model of the landslides and debris flows in the Southern Andes, suggesting areas prone to such occurrences and should be monitored closely to develop effective mitigation strategies.

7 Code availability

All the codes used in this manuscript are reproducible from the main text. We can to deliver the main script under any request.

8 Data availability

The datasets used in this study are available in the paper. The ALOS-PALSAR DEM is publicly accessible at https://search.asf.alaska.edu/#/?dataset=ALOS (last access: 30 September 2024). Additional information about the information or datasets can be obtained from Ivo Janos Fustos-Toribio, ivo.fustos@ufrontera.cl.

9 Author contributions

IF, DB and AG contributed to the conceptualisation and methodology of the research and performed the formal analysis, visualisation and validation. IF and DB were involved in the funding and supervision of the paper. IF and AB contributed with the supervision, review and editing of the paper. SS contributed to the discussion of the scientific results. All the authors provided input in terms of methodology and the review and editing of the paper.

https://doi.org/10.5194/egusphere-2025-1394
Preprint. Discussion started: 9 April 2025

10 Competing interests

The authors declare that they have no conflict of interest.

11 Disclaimer

12 Acknowledgements

This work was made possible thanks to the "Agencia Nacional de Investigación y Desarrollo (ANID)" of the Chilean Government; "Fondecyt Regular" grant 1230792); "Fondecyt post-doctoral" grant 3200387) and CIVUR-39° "Centro Interactivo Vulcanológico de La Araucania" Project FRO2193 of the Desarrollo de Actividades de Interes Nacional (ADAIN), Ministry of Education, Chilean Government. We appreciate the support of Mauricio Hermosilla for their support in geotechnical analysis.

13 Financial support

This research has been supported by ANID (grant nos. Fondecyt 3200387 and Fondecyt 1230792).

14 References

Bekaert, D. P. S., Walters, R. J., Wright, T. J., Hooper, A. J., und Parker, D. J.: Statistical comparison of InSAR tropospheric correction techniques, Remote Sensing of Environment, 170, 40–47, doi: 10.1016/j.rse.2015.08.035, 2015.

Blasco, J. M. D. und Foumelis, M.: Automated SNAP Sentinel-1 DInSAR processing for StaMPS PSI with open source tools, Zenodo, doi: 10.5281/ZENODO.1322353, 2018.

Bogaard, T. A. und Greco, R.: Landslide hydrology: from hydrology to pore pressure, WIREs Water, 3, 439–459, doi: 10.1002/wat2.1126, 2015.

Bordoni, M., Vivaldi, V., Ciabatta, L., Brocca, L., und Meisina, C.: Temporal prediction of shallow landslides exploiting soil saturation degree derived by ERA5-Land products, Bull Eng Geol Environ, 82, doi: 10.1007/s10064-023-03304-2, 2023.

Bucher, J., del Papa, C., Hernando, I. R., und Almada, G.: Upper-flow-regime deposits related to glacio-volcanic interactions in Patagonia: Insights from the Pleistocene record in Southern Andes, Sedimentology, doi: 10.1111/sed.13216, 2024.

Chen, Y., Lin, H., Cao, R., und Zhang, C.: Slope Stability Analysis Considering Different Contributions of Shear Strength Parameters, Int. J. Geomech., 21, doi: 10.1061/(asce)gm.1943-5622.0001937, 2021.

https://doi.org/10.5194/egusphere-2025-1394
Preprint. Discussion started: 9 April 2025

Carrasco Felipe and Ramírez Paola: Caracterización de remociones en masa del 31 de mayo de 2021, en la ribera sur del Lago Calafquén, sobre la Ruta CH-201, Comuna de Panguipulli, Región de Los Ríos. Informe inédito. INF-LOS RÍOS-09.2021. 2021. Subdirección Nacional De Geología, Sernageomin, Stgo, Chile. PP:23.

Chang, J.-M., Chen, H., Jou, B. J.-D., Tsou, N.-C., und Lin, G.-W.: Characteristics of rainfall intensity, duration, and kinetic energy for landslide triggering in Taiwan, Engineering Geology, 231, 81–87, doi: 10.1016/j.enggeo.2017.10.006, 2017.

Cheung, D. J. und Giardino, J. R.: Debris flow occurrence under changing climate and wildfire regimes: A southern California perspective, Geomorphology, 422, 108538, doi: 10.1016/j.geomorph.2022.108538, 2023.

Dahal, R. K. und Hasegawa, S.: Representative rainfall thresholds for landslides in the Nepal Himalaya, Geomorphology, 100, 429–443, doi: 10.1016/j.geomorph.2008.01.014, 2008.

Dahal, R. K., Hasegawa, S., Yamanaka, M., und Bhandary, N. P.: Rainfall-induced landslides in the residual soil of andesitic terrain, western Japan, Journal of Nepal Geological Society, 42, 137–152, doi: 10.3126/jngs.v42i0.31461, 2011.

Dane, H. Topp, G., 2002. Methods of Soil Analysis Part-4 Physical Methods.

Dey, N. und Sengupta, A.: Effect of rainfall on the triggering of the devastating slope failure at Malin, India, Nat Hazards, 94, 1391–1413, doi: 10.1007/s11069-018-3483-9, 2018.

De Pue, J., Rezaei, M., Van Meirvenne, M., und Cornelis, W. M.: The relevance of measuring saturated hydraulic conductivity: Sensitivity analysis and functional evaluation, Journal of Hydrology, 576, 628–638, doi: 10.1016/j.jhydrol.2019.06.079, 2019.

Ferretti, A., Prati, C., und Rocca, F.: Permanent scatterers in SAR interferometry, IEEE Trans. Geosci. Remote Sensing, 39, 8–20, doi: 10.1109/36.898661, 2001.

Fontaine, C. M., Siani, G., Delpech, G., Michel, E., Villarosa, G., Manssouri, F., und Nouet, J.: Post–glacial tephrochronology record off the Chilean continental margin (~41° S), Quaternary Science Reviews, 261, 106928, doi: 10.1016/j.quascirev.2021.106928, 2021.

Foumelis, M., Delgado Blasco, J. M., Desnos, Y.-L., Engdahl, M., Fernandez, D., Veci, L., Lu, J., und Wong, C.: Esa Snap - Stamps Integrated Processing for Sentinel-1 Persistent Scatterer Interferometry, IGARSS 2018 - 2018 IEEE International Geoscience and Remote Sensing Symposium, doi: 10.1109/igarss.2018.8519545, 2018.

Funk, C., Peterson, P., Landsfeld, M., Pedreros, D., Verdin, J., Shukla, S., Husak, G., Rowland, J., Harrison, L., Hoell, A., und Michaelsen, J.: The climate hazards infrared precipitation with stations—a new environmental record for monitoring extremes, Sci Data, 2, doi: 10.1038/sdata.2015.66, 2015.

Fustos, I., Abarca-del-Rio, R., Ávila, A., und Orrego, R.: A simple logistic model to understand the occurrence of flood events into the Biobío River Basin in central Chile, J Flood Risk Management, 10, 17–29, doi: 10.1111/jfr3.12131, 2014.

Fustos, I., Remy, D., Abarca-Del-Rio, R., und Muñoz, A.: Slow movements observed within situand remote-sensing techniques in the central zone of Chile, International Journal of Remote Sensing, 38, 7514–7530, doi: 10.1080/01431161.2017.1317944, 2017.

Fustos, I., Abarca-del-Rio, R., Moreno-Yaeger, P., und Somos-Valenzuela, M.: Rainfall-Induced Landslides forecast using local precipitation and global climate indexes, Nat Hazards, 102, 115–131, doi: 10.1007/s11069-020-03913-0, 2020.

https://doi.org/10.5194/egusphere-2025-1394
Preprint. Discussion started: 9 April 2025

Fustos, I., Abarca-del-Río, R., Mardones, M., González, L., und Araya, L. R.: Rainfall-induced landslide identification using numerical modelling: A southern Chile case, Journal of South American Earth Sciences, 101, 102587, doi: 10.1016/j.jsames.2020.102587, 2020.

Fustos-Toribio, I. J., Morales-Vargas, B., Somos-Valenzuela, M., Moreno-Yaeger, P., Muñoz-Ramirez, R., Rodriguez Araneda, I., und Chen, N.: Debris flow event on Osorno volcano, Chile, during summer 2017: new interpretations for chain processes in the southern Andes, Nat. Hazards Earth Syst. Sci., 21, 3015–3029, doi: 10.5194/nhess-21-3015-2021, 2021.

Fustos-Toribio, I., Manque-Roa, N., Vásquez Antipan, D., Hermosilla Sotomayor, M., und Letelier Gonzalez, V.: Rainfall-induced landslide early warning system based on corrected mesoscale numerical models: an application for the southern Andes, Nat. Hazards Earth Syst. Sci., 22, 2169–2183, doi: 10.5194/nhess-22-2169-2022, 2022.

Hooper, A., Segall, P., und Zebker, H.: Persistent scatterer interferometric synthetic aperture radar for crustal deformation analysis, with application to Volcán Alcedo, Galápagos, J. Geophys. Res., 112, doi: 10.1029/2006jb004763, 2007.

Hirschberg, J., Fatichi, S., Bennett, G. L., McArdell, B. W., Peleg, N., Lane, S. N., Schlunegger, F., und Molnar, P.: Climate Change Impacts on Sediment Yield and Debris-Flow Activity in an Alpine Catchment, JGR Earth Surface, 126, doi: 10.1029/2020jf005739, 2021.

Höser, T.: Analysing the Capabilities and Limitations of InSAR using Sentinel-1 Data for Landslide Detection and Monitoring, Unpublished, doi: 10.13140/RG.2.2.35085.59362, 2018.

Huang, A.-B., Lee, J.-T., Ho, Y.-T., Chiu, Y.-F., und Cheng, S.-Y.: Stability monitoring of rainfall-induced deep landslides through pore pressure profile measurements, Soils and Foundations, 52, 737–747, doi: 10.1016/j.sandf.2012.07.013, 2012.

Hungr, O., Leroueil, S., und Picarelli, L.: The Varnes classification of landslide types, an update, Landslides, 11, 167–194, doi: 10.1007/s10346-013-0436-y, 2014.

Jakob, M. und Lambert, S.: Climate change effects on landslides along the southwest coast of British Columbia, Geomorphology, 107, 275–284, doi: 10.1016/j.geomorph.2008.12.009, 2009.

Kinde, M., Getahun, E., und Jothimani, M.: Geotechnical and slope stability analysis in the landslide-prone area: A case study in Sawla – Laska road sector, Southern Ethiopia, Scientific African, 23, e02071, doi: 10.1016/j.sciaf.2024.e02071, 2024.

Korup, O., Seidemann, J., und Mohr, C. H.: Increased landslide activity on forested hillslopes following two recent volcanic eruptions in Chile, Nat. Geosci., 12, 284–289, doi: 10.1038/s41561-019-0315-9, 2019.

Lee, C.-T.: Landslide trends under extreme climate events, Terr. Atmos. Ocean. Sci., 28, 33–42, doi: 10.3319/tao.2016.05.28.01(cca), 2017.

Maragaño-Carmona, G., Fustos Toribio, I. J., Descote, P.-Y., Robledo, L. F., Villalobos, D., und Gatica, G.: Rainfall-Induced Landslide Assessment under Different Precipitation Thresholds Using Remote Sensing Data: A Central Andes Case, Water, 15, 2514, doi: 10.3390/w15142514, 2023.

Moreno-Yaeger, P., Singer, B. S., Edwards, B. R., Jicha, B. R., Nachlas, W. O., Kurz, M. D., E. Breunig, R., Fustos-Toribio, I., Antipán, D. V., and Piergrossi, E.: Pleistocene to recent evolution of Mocho-Choshuenco volcano during growth and retreat of the Patagonian Ice Sheet, Geological Society of America Bulletin, 136, 5262–5282, doi: 10.1130/b37514.1, 2024.

https://doi.org/10.5194/egusphere-2025-1394
Preprint. Discussion started: 9 April 2025

Muñoz-Sabater, J., Dutra, E., Agustí-Panareda, A., Albergel, C., Arduini, G., Balsamo, G., Boussetta, S., Choulga, M., Harrigan, S., Hersbach, H., Martens, B., Miralles, D. G., Piles, M., Rodríguez-Fernández, N. J., Zsoter, E., Buontempo, C., und Thépaut, J.-N.: ERA5-Land: a state-of-the-art global reanalysis dataset for land applications, Earth Syst. Sci. Data, 13, 4349–4383, doi: 10.5194/essd-13-4349-2021, 2021.

Muratli, J. M., Chase, Z., McManus, J., und Mix, A.: Ice-sheet control of continental erosion in central and southern Chile (36°–41°S) over the last 30,000 years, Quaternary Science Reviews, 29, 3230–3239, doi: 10.1016/j.quascirev.2010.06.037, 2010.

Ontiveros-Ortega, A., Plaza, I., Calero, J., Moleon, J. A., und Ibañez, J. M.: High variability of interaction energy between volcanic particles: implications for deposit stability, Nat Hazards, 117, 3103–3122, doi: 10.1007/s11069-023-05979-y, 2023.

Palazzolo, N., Peres, D. J., Creaco, E., und Cancelliere, A.: Using principal component analysis to incorporate multi-layer soil moisture information in hydrometeorological thresholds for landslide prediction: an investigation based on ERA5-Land reanalysis data, Nat. Hazards Earth Syst. Sci., 23, 279–291, doi: 10.5194/nhess-23-279-2023, 2023.

Porchet M. and Laferrere H. Détermination des caractéristiques hydrodynamiques des sols en place. Mémoire et notes techniques. Ann. Du Ministère de l'Agriculture, Tech. Rep. 2 (64), 1935.

Rawson, H., Naranjo, J. A., Smith, V. C., Fontijn, K., Pyle, D. M., Mather, T. A., und Moreno, H.: The frequency and magnitude of post-glacial explosive eruptions at Volcán Mocho-Choshuenco, southern Chile, Journal of Volcanology and Geothermal Research, 299, 103–129, doi: 10.1016/j.jvolgeores.2015.04.003, 2015.

Rodriguez, C., Perez, Y., Hugo Roa, Clayton, J., Antinao, J. L., & Duhart, P., Martin, M.: Geología del área de Panguipulli-Riñihue, Región de Los Lagos. Servicio Nacional de Geología y Minería, Mapas Geológicos No: 10. 1999.

SANHUEZA, C., PALMA, J., VALENZUELA, P., ARANEDA, O., und CALDERÓN, K.: Evaluación del comportamiento geotécnico de suelos volcánicos chilenos para su uso como material de filtro en la depuración de aguas residuales domésticas, Revista de la Construcción, 10, 66–81, doi: 10.4067/s0718-915x2011000200007, 2011.

Sepúlveda, S. A., Rebolledo, S., und Vargas, G.: Recent catastrophic debris flows in Chile: Geological hazard, climatic relationships and human response, Quaternary International, 158, 83–95, doi: 10.1016/j.quaint.2006.05.031, 2006.

Sepúlveda, S. A. und Petley, D. N.: Regional trends and controlling factors of fatal landslides in Latin America and the Caribbean, Nat. Hazards Earth Syst. Sci., 15, 1821–1833, doi: 10.5194/nhess-15-1821-2015, 2015.

Singer, B. S., Moreno-Yaeger, P., Townsend, M., Huber, C., Cuzzone, J., Edwards, B. R., Romero, M., Orellana-Salazar, Y., Marcott, S. A., Breunig, R. E., Ferrier, K. L., Scholz, K., Coonin, A. N., Alloway, B. V., Tremblay, M. M., Stevens, S., Fustos-Toribio, I., Moreno, P. I., Vera, F., und Amigo, Á.: New perspectives on ice forcing in continental arc magma plumbing systems, Journal of Volcanology and Geothermal Research, 455, 108187, doi: 10.1016/j.jvolgeores.2024.108187, 2024.

Singh, K. und Kumar, V.: Rainfall Thresholds Triggering Landslides: A Review, Lecture Notes in Civil Engineering, 455–464, doi: 10.1007/978-3-030-51354-2_42, 2020.

https://doi.org/10.5194/egusphere-2025-1394
Preprint. Discussion started: 9 April 2025

Somos-Valenzuela, M. A., Oyarzún-Ulloa, J. E., Fustos-Toribio, I. J., Garrido-Urzua, N., und Chen, N.: The mudflow disaster at Villa Santa Lucía in Chilean Patagonia: understandings and insights derived from numerical simulation and postevent field surveys, Nat. Hazards Earth Syst. Sci., 20, 2319–2333, doi: 10.5194/nhess-20-2319-2020, 2020.

Stern, C. R.: Active Andean volcanism: its geologic and tectonic setting, Rev. geol. Chile, 31, doi: 10.4067/s0716-02082004000200001, 2004.

Thompson, P. I. J., Dugmore, A. J., Newton, A. J., Cutler, N. A., und Streeter, R. T.: The influence of burial rate on variability in tephra thickness and grain size distribution in Iceland, CATENA, 225, 107025, doi: 10.1016/j.catena.2023.107025, 2023.

Usai, S.: A least squares database approach for SAR interferometric data, IEEE Trans. Geosci. Remote Sensing, 41, 753–760, doi: 10.1109/tgrs.2003.810675, 2003.

Valenzuela, R. A. and Garreaud, R. D.: Extreme Daily Rainfall in Central-Southern Chile and Its Relationship with Low-Level Horizontal Water Vapor Fluxes, Journal of Hydrometeorology, 20, 1829–1850, doi: 10.1175/jhm-d-19-0036.1, 2019.

Vega, J. A. and Hidalgo, C. A.: Quantitative risk assessment of landslides triggered by earthquakes and rainfall based on direct costs of urban buildings, Geomorphology, 273, 217–235, doi: 10.1016/j.geomorph.2016.07.032, 2016.

Veci L, Lu J, Prats-Iraola P, Scheiber R, Collard F, Fomferra N, Engdahl M.: The Sentinel-1 Toolbox. In: Proceedings of the IEEE International Geoscience and Remote Sensing Symposium (IGARSS); 13– Quebec City, QC, Canada, 18 July 2014. p. 1–3. 2014.

Walding, N., Williams, R., Rowley, P., und Dowey, N.: Cohesional behaviours in pyroclastic material and the implications for deposit architecture, Bull Volcanol, 85, doi: 10.1007/s00445-023-01682-9, 2023.

Wang, H., Cui, P., Li, Y., Tang, J., Wei, R., Yang, A., Zhou, L., Bazai, N. A., und Zhang, G.: Rock and ice avalanche-generated catastrophic debris flow at Chamoli, 7 February 2021: New insights from the geomorphic perspective, Geomorphology, 452, 109110, doi: 10.1016/j.geomorph.2024.109110, 2024.

Xie, M., Zhao, W., Ju, N., He, C., Huang, H., und Cui, Q.: Landslide evolution assessment based on InSAR and real-time monitoring of a large reactivated landslide, Wenchuan, China, Engineering Geology, 277, 105781, doi: 10.1016/j.enggeo.2020.105781, 2020.

Yi, Z., Xingmin, M., Allesandro, N., Tom, D., Guan, C., Colm, J., Yuanxi, L., und Xiaojun, S.: Characterization of pre-failure deformation and evolution of a large earthflow using InSAR monitoring and optical image interpretation, Landslides, 19, 35–50, doi: 10.1007/s10346-021-01744-z, 2021.

Yu, C., Li, Z., Penna, N. T., und Crippa, P.: Generic Atmospheric Correction Model for Interferometric Synthetic Aperture Radar Observations, JGR Solid Earth, 123, 9202–9222, doi: 10.1029/2017jb015305, 2018.